Electronic Supplementary Information

Mo-modified electronic effect on Sub-2 nm Ru catalyst for enhancing the hydrogen oxidation catalysis

Min Ma,[a,b] Chaofan Chen,[a] Xibo Zhang,[a] Hongsheng Zhao,[a] Qiuxiang Wang,[c] Guifen Du,[c] ZhaoxiongXie,[a] and Qin Kuang[a*]

[a] State Key Laboratory of Physical Chemistry of Solid Surfaces & Department of Chemistry, College of Chemistry and Chemical Engineering, Xiamen University, Xiamen 361005, Fujian (P. R. China). E-mail: qkuang@xmu.edu.cn; Fax: (+) 86-592-2183047.

[b] School of Materials Science and Engineering, Shandong University of Science and Technology, Qingdao 266590, Shandong(P. R. China).

[c] Instrumental Analysis Center, Huaqiao University, Xiamen 361021, Fujian (P. R. China).

1. Experimental Section

Materials: *:*Zinc nitrate hexahydrate ($Zn(NO_3)_2 \cdot 6H_2O$, 99%), potassium hydroxide (KOH, ≥85%), sulfuric acid (H_2SO_4, 95~98%), methanol (CH_3OH, ≥99.5%), ethanol (C_2H_5OH, ≥99.7%) were purchased from Sinopharm Chemical Reagent Co. Ltd. (Shanghai, China).Phosphomolybdic acid (PMA, $H_3[P(Mo_3O_{10})_4] \cdot xH_2O$) was purchased from Tianjin Guangfu Fine Chemical Research Institute, and $RuCl_3 \cdot xH_2O$ was provided by Aladdin Reagent (Shanghai) Co., Ltd. Ru/C (5 wt%) was provided by Alfa Aesar (China) Chemicals Co., Ltd. whlie 2-methylimidazole (HmIM, 99%）was supplied by J.K. Ultra-high purity H_2 (UHP, >99.999%) and ultra-high purity Ar (UHP, >99.999%) were purchased from Linde Industrial Gases.

Preparation of Ru/C working electrodes: Firstly, 2 mg of Ru/C were dispersed in the mixed solution containing of 350 μL C_3H_8O, 140 μL H_2O and 10 μL Nafion. To obtain a homogeneous ink, the forcefully ultrasonicated process was performed on this aforesaid solution for at least 2 h. This calculated ink was then carefully coated onto the clean glassy carbon electrode (GC). It should be noted that GC electrode was set at the rotating speed of 800 rpm to prepare the uniform catalyst film having a Ru loading of 15.0 μg cm^{-2}. The preparation for other working electrodes, such as Sub-2 nm RuMo/HC (Ru loading of 13.3 μg cm^{-2}), Sub-2 nm Ru/HC (Ru loading of 14.7 μg cm^{-2}) and Pt/C, also followed this above process.

Characterizations: X-ray diffraction (XRD) patterns of our samples were operated on a Rigaku Ultima IV diffractometer with Cu Kαradiation (40 KV, 30 mA). Scanning electron microscope (SEM) images were collected on a Hitachi S4800 device at an accelerated voltage (15 kV), while X-ray photoelectron spectroscopy (XPS) and its valence band spectra were measured on an ESCALab 250 X-ray photoelectron spectrometer. Transmission electron microscope (TEM), high angle annular fark-field scanning TEM (HAADF-STEM), and energy dispersive X-ray (EDX) elemental mapping images were recorded on an FEI TECNAI F30 microscope with an accelerating voltage of 300 KV. The quantitative analysis of metal elements in samples were achieved by inductively coupled plasma optical emission spectrometry (ICP-OES). And before the ICP-OES test, sample powder needed to be digested in aqua regia (HCl/HNO$_3$ =3:1) for at least 6 times.

Electrochemical measurement: Electrochemical tests were performed on rotating ring disk electrode (RRDE-3A，ALS) and CHI 650E electrochemical workstation (CH Instruments, Inc., Shanghai) in 0.1 M KOH under ambiet conditions. A typical three-electrode system was utilized to estimate the alkaline HOR performance on as-studied catalysts, where Sub-2 nm RuMo/HC(or other control samples) was used as the working electrode, carbon rod as the counter electrode, and saturated calomel electrode (SCE) as the

reference electrode. Before HOR test, cyclic voltammetry (CV) for over 20 cycles were performed to clean and activate the electrode's surface. Then, the HOR activities were measured by linear sweep voltammetry (LSV) with a positive scan rate of 10 mV s^{-1} in H$_2$-saturated 0.1 M KOH (rotating speed: 1600 rpm). Especially, electrical resistance (iR) compensation for all catalysts was corrected automatically during HOR testing on electrochemical workstation.

Calculation of d band center: To reveal the effect of Mo element on the electronic structure of Ru surface, XPS valence band spectra of three samples were measured and analyzed. As previously reported, the position of d band center (ε_d) from XPS valence band spectra could be obtained from the next formula:

$$\varepsilon_d = \frac{\int \rho \, E dE}{\int \rho dE}$$

Where ρ and E are the density of states and energy of electron, respectively. It should be noted that the intensity in XPS valence-band spectra is proportional to the density of states.
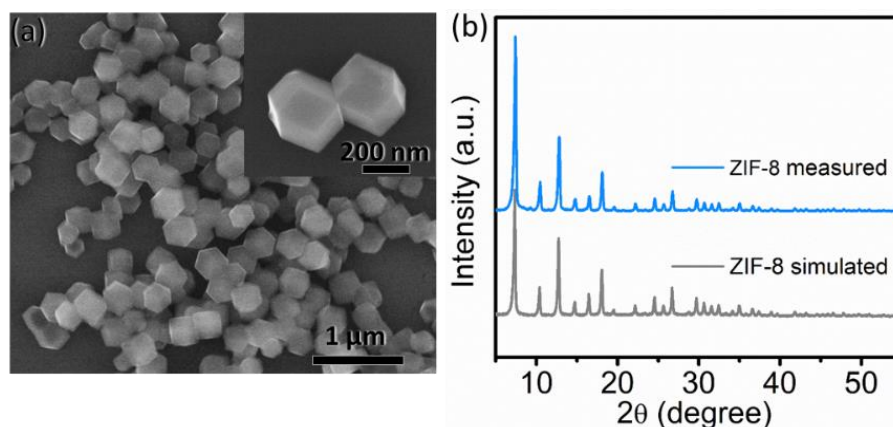
2. Supplementary Results

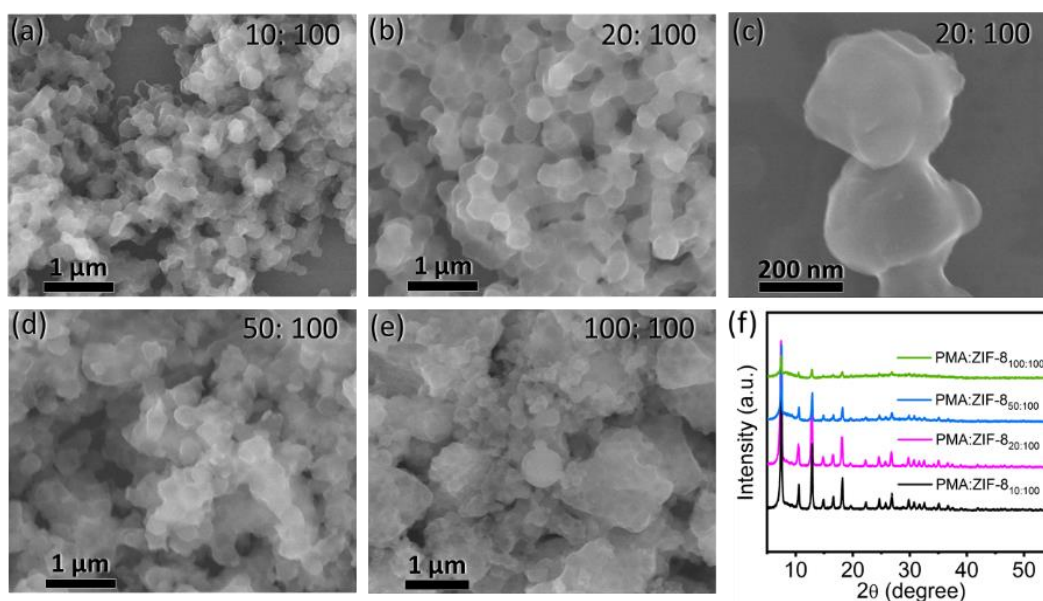**Fig. S1** (a) SEM images and (b) measured and simulated XRD patterns of ZIF-8 sample.

Fig. S2 (a-e) SEM images and (f) XRD patterns of ZIF-8@Mo precursors with different mass ratios of ZIF-8/PMA raw material.
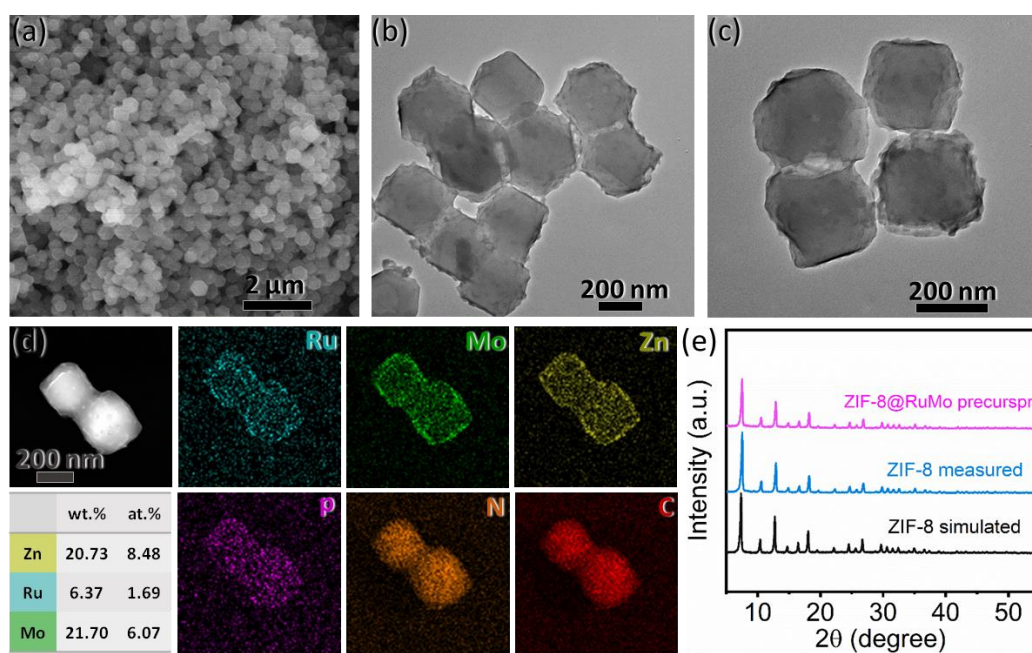

Fig. S3 (a) SEM and (b-c) TEM images of ZIF-8@RuMo precursor. (d) HAADF-STEM image and corresponding element mapping images of ZIF-8@RuMo precursor. (e) XRD patterns of ZIF-8@RuMo precursor and ZIF-8 (measured/simulated).
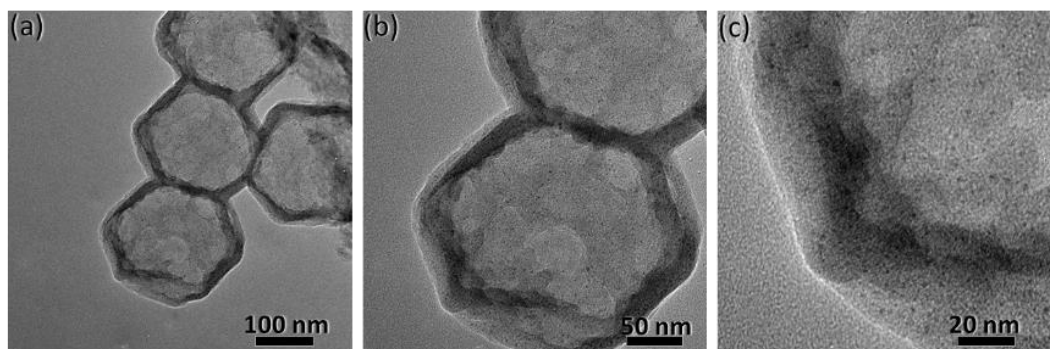
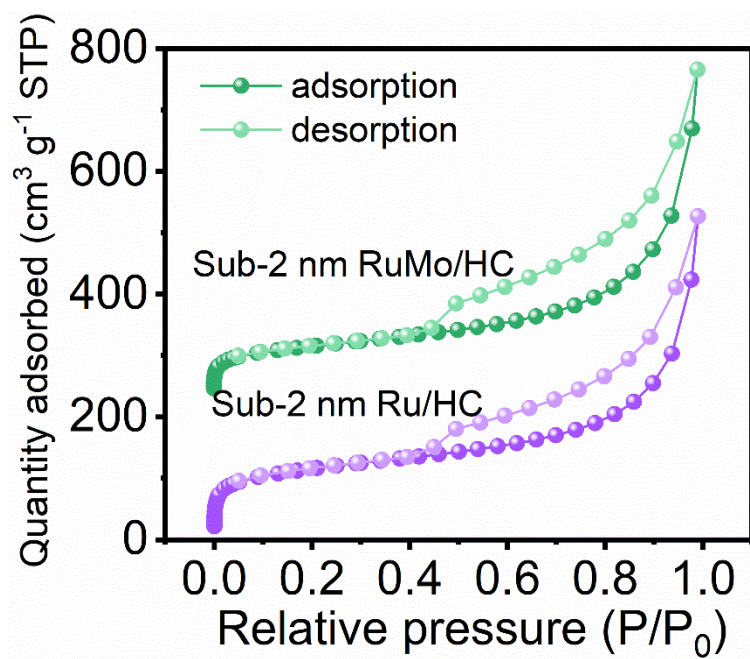**Fig. S4** TEM and HR-TEM images of Sub-nm Ru/NHC at different magnifications.

Fig. S5 N_2 adsorption-desorption isotherms of Sub-2 nm RuMo/HC and Sub-2 nm Ru/HC.
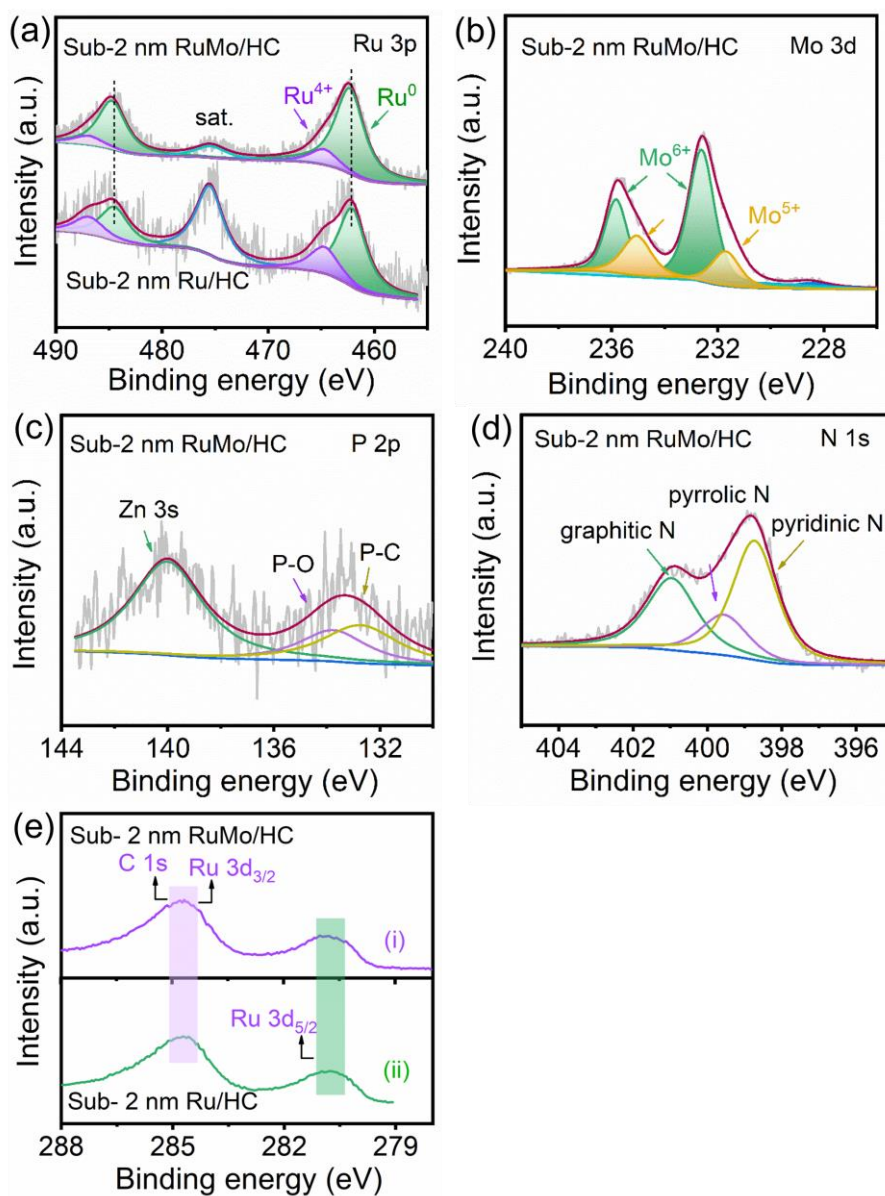
Fig. S6 XPS spectra in the (a) Ru 3p, (b) Mo 3d, (c) P 2p, (d) N 1s and (e) C 1s or Ru 3d regions from Sub-2 nm RuMo/HC or Sub-2 nm Ru/HC catalysts.
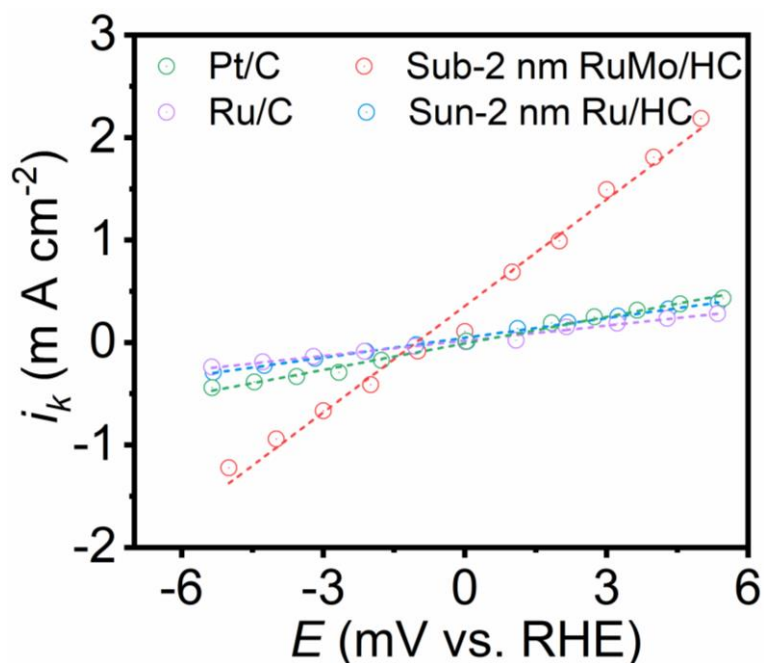
Fig. S7 Micro-polarization region curves for Sub-2 nm RuMo/HC, Sub-2 nm Ru/HC, commercial Ru/C and Pt/C catalysts. The dotted lines represent the fitting ones.
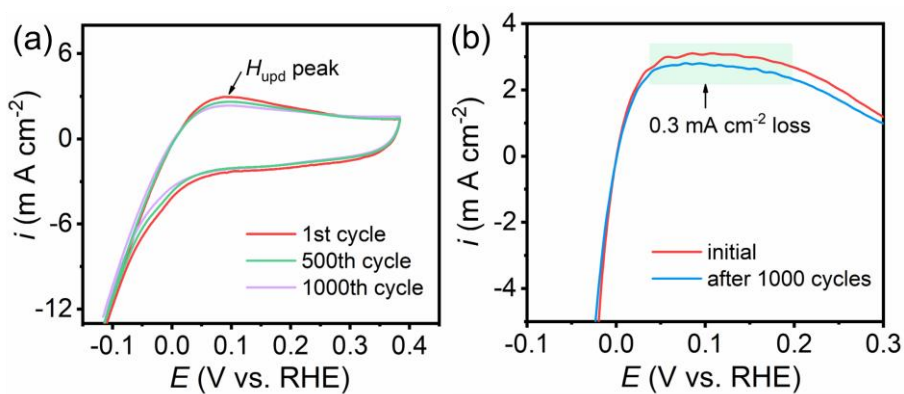

Fig. S8 (a) CV curves of Sub-2 nm RuMo/HC at different cycles with a scan rate of 50 mV s^{-1}, and (b) comparison of the LSV curves for Sub-2 nm RuMo/HC before and after 1000 cycles tested in H$_2$-saturated 0.1 M KOH.
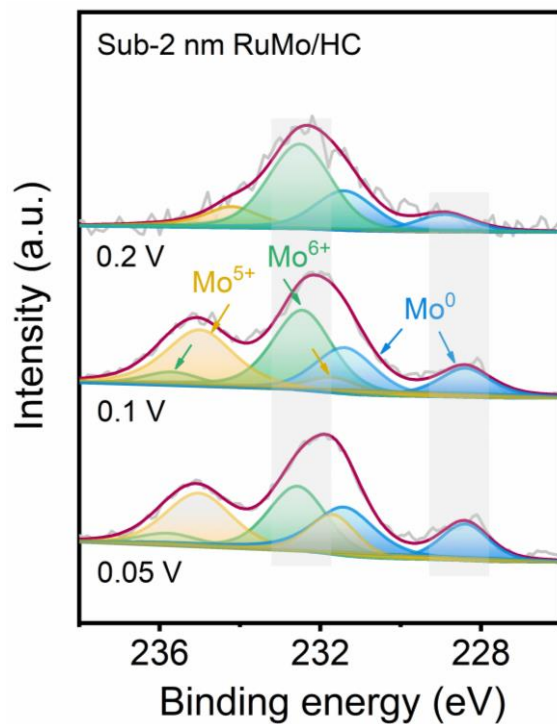
Fig. S9 XPS spectra in the Mo 3d region from Sub-2 nm RuMo/HC after stability test under different applied potentials from 0.05 to 0.20 V vs. RHE.

Table S1 EDX data of Sub-2 nm RuMo/HC and Sub-2 nm Ru/HC samples.

Element	Sub-2 nm RuMo/HC (wt.%)	Sub-2 nm Ru/HC (wt.%)
Ru	20.93	16.01
Mo	32.75	~~
C	38.49	74.28
N	2.06	3.53
P	1.03	~~
O	4.74	6.18

Table S2 ICP data of Sub-2 nm RuMo/HC and Sub-2 nm Ru/HC samples.

Sample	Data 1 (wt.%)	Data 2 (wt.%)	Data 3 (wt.%)	Average (wt.%)
Sub-2 nm RuMo/HC	18.59 (Ru)	18.54 (Ru)	18.63 (Ru)	18.59 (Ru)
Sub-2 nm RuMo/HC	28.78 (Mo)	28.71 (Mo)	28.64 (Mo)	28.71 (Mo)
Sub-2 nm Ru/HC	15.75 (Ru)	15.70 (Ru)	15.58 (Ru)	15.67 Ru)

Table S3 Comparison for exchange current density (j_0) and transfer coefficient (α) of Sub-2 nm RuMo/HC, Sub-2 nm Ru/HC, commercial Pt/C and Ru/C samples.

Catalyst	j_0 (mA cm^{-2})[a]	Transfer coefficients (α)	j_0 (mA cm^{-2})[b]
Sub-2 nm RuMo/HC	10.3	0.76	8.91
Sub-2 nm Ru/HC	1.71	0.54	1.65
Pt/C	1.90	0.56	2.22
Ru/C	1.16	0.45	1.27

j_0 (mA cm^{-2})[a]:The j_0 value is calculated by non-linear fitting of theTafel plot with Butler−Volmer equation;

j_0 (mA cm^{-2})[b]: The j_0 value is determined by linear fitting of the micro−polarized region.

Table S4 Comparisons of HOR performance for as-prepared Sub-2 nm RuMo/HC and Sub-2 nm Ru/HC with other Ru-based catalysts operated in alkaline electrolyte.

Catalyst	η mV@*MA*	loading	Ref.
Sub-2 nm RuMo/HC	50@3.83 A mg^{-1}PGM 20@0.81 A mg^{-1}PGM	13.3 µgPGM cm^{-2}	This work
Sub-2 nm Ru/HC	50@0.30 A mg^{-1}PGM	14.7 µgPGM cm^{-2}	This work
Ru@TiO$_2$	20@<0.3 A mg^{-1}PGM	25 µgPGM cm^{-2}	*Nat. Catal.* 2020, **3**, 454–462.
Ru$_7$Ni$_3$/C	50@9.4 A mg^{-1}PGM	3.9 µgPGM cm^{-2}	*Nat. Commun.* 2020, **11**,565.
RuNi1	50@2.7 A mg^{-1}PGM	~8 µgPGM cm^{-2}	*Nano Lett.* 2020, **20**, 3442–3448.
Ru$_{0.95}$Co$_{0.05}$/C	10@0.16 A mg^{-1}PGM	~13 µgPGMcm^{-2}	*ACS Catal.* 2020, **10**, 4608−4616.
P−Ru/C	~~	~6 µgPGMcm^{-2}	*ACS Catal.* 2020, **10**, 11751−11757.
Ru nanoassembly	50@0.041 A mg^{-1}PGM	180 µgPGMcm^{-2}	*Appl. Catal. B* 2019, **258**, 117952.
Ru/PEI-XC	50@0.423 A mg^{-1}PGM	~21.6 µgPGMcm^{-2}	*J. Mater. Chem. A* 2021, **9**, 22934–22942.
RuRh-Co	50@0.0117 A mg^{-1}PGM	250 µgmetalcm^{-2}	*Nano Energy* 2021, **90**, 106579.
IO-Ru–TiO$_2$/C	50@0.907 A mg^{-1}PGM	25.48 µgPGMcm^{-2}	*J. Mater. Chem. A* 2020, **8**, 10168–10174.

Table S5 Percentage content of RuO_x (Ru^{4+}) on two samples' surface after electrolysis test at different overpotential. These data were calculated from Ru 3p XPS spectra.

Catalyst	0.05 V vs. RHE	0.1 V vs. RHE	0.2 V vs. RHE
Sub-2 nm RuMo/HC	9.9%RuO_x	11.7%RuO_x	12.6%RuO_x
Sub-2 nm Ru/HC	23.5%RuO_x	27.3%RuO_x	40.9%RuO_x